

Simulation of Natural Convection Heat Transfer in a 2-D Trapezoidal Enclosure

K. Venkatadri¹, S. Abdul Gaffar^{2*}, V. R. Prasad³, B. Md. Hidayathualla Khan⁴
and O. A. Beg⁵

¹Department of Mathematics, VEMU Institute of Technology, P.Kothakota-517112,
India

²Department of Information Technology, Mathematics Section, Salalah College of
Technology, Salalah - 211, Oman.

*Email: abdulgaffar0905@gmail.com

Phone No: +96890441522

³Department of Mathematics, School of Advanced Sciences, Vellore Institute of
Technology, Vellore – 6322014, India

⁴Department of Mathematics, Sir Vishveshwaraiah Institute of Science and Technology,
Madanapalle- 517325, India

⁵Magnetohydrodynamics, Biological Propulsion and Energy Research, Aeronautical and
Mechanical Engineering Division, University of Salford, M5 4WT, UK

ABSTRACT

Natural convection within trapezoidal enclosures finds significant practical applications. The natural convection flows play a prominent role in the transport of energy in energy-related applications, in case of proper design of enclosures to achieve higher heat transfer rates. In the present study, a two-dimensional cavity with adiabatic right side wall is studied. The left side vertical wall is maintained at the constant hot temperature and the top slat wall is maintained at cold temperature. The dimensionless governing partial differential equations for vorticity-stream function are solved using the finite difference method with incremental time steps. The parametric study involves a wide range of Rayleigh number, Ra , $10^3 \leq Ra \leq 10^5$ and Prandtl number ($Pr = 0.025, 0.71$ and 10). The fluid flow within the enclosure is formed with different shapes for different Pr values. The flow rate is increased by enhancing the Rayleigh number ($Ra = 10^4$). The numerical results are validated with previous results. The governing parameters in the present article, namely Rayleigh number and Prandtl number on flow patterns, isotherms as well as local Nusselt number are reported.

Keywords: Natural convection; trapezoidal enclosure; finite difference method; incompressible flow; explicit time integration.

INTRODUCTION

The finite spaces bounded by walls and filled with fluid are termed as enclosures. The internal natural convection also termed as natural convection within enclosures, usually takes place in rooms and buildings, furnaces, cooling towers and electronic cooling systems. The internal natural convection has been studied widely using various analytical, numerical and experimental techniques due to its wide range of applications in engineering technology such as nuclear reactor system, double pane windows, microelectromechanical systems (MEMS), cooling of electronic devices, solar thermal collectors and so on [1]. Heat transfer enhancement in such systems is essential given

energy-saving perspective and proper functionality of the devices. The natural convection analysis within closed cavities has gained significant attention and finds applications in fluid flow geothermal reservoirs, solidification of casting, solar energy collectors, sterilisation, food separation processes, molten metal applications, and molten salt applications and so on. Iyican [2–3] presented a two-dimensional circulation based model to study the heat transfer analysis in a trapezoidal enclosure with adiabatic sidewalls. Iyican and Bayazitoglu [4] experimentally presented the natural convection of air in an inclined trapezoidal enclosure with Rayleigh number ranging from $\sim 2 \times 10^3$ to $\sim 5 \times 10^7$.

An extensive analysis of heatlines is presented by Basak et al. [5] to study the heat flow patterns of various trapezoidal cavities. They presented the heat functions and stream functions along with velocity and temperature profiles using Galerkin finite difference method. Esfe et al. [6] explored the natural convection flow and heat transfer of CNT-EG-water nanofluid in a trapezoidal enclosure. Muneer and Chamkha [7] used the under successive relaxation upwind-scheme finite difference method to analyse the laminar convection inside a square composite vertically layered porous cavity with a nanofluid. Chamkha and Hameed [8] analysed the double-diffusive convection flow due to opposing temperature and concentration gradients of an electrically conducting and heat-generating or absorbing fluid inside a rectangular enclosure with uniform side heat and mass fluxes in the presence of a transverse magnetic field using the finite difference technique. Nakhi and Chamkha [9] implemented the finite volume technique to numerically study the conjugate natural convection heat transfer in a square enclosure with three thick cooled walls and one thin heated vertical wall with a heated inclined thin fin attached in middle. They observed that the thin fin inclination angle and length and solid to fluid thermal conductivity ratio have significant effects on the local and average Nusselt number at the heated surfaces of the enclosure/fin system.

Mixed convection flow numerical model of Cu)-Water nanofluid in a differentially heated lid-driven cavity with a bottom wavy wall was presented by Nada and Chamkha [10]. They observed that the presence of nanoparticle produces significant heat transfer augmentation for an increase in Richardson number. Chamkha [11] used the finite-difference method to study the double-diffusive convective flow of a binary gas-particle mixture inside a rectangular porous enclosure with cooperating temperature and concentration gradients in the presence of heat generation or absorption effects. He observed that the heat and mass transfer characteristics inside the enclosure depended strongly on the inverse Darcy number and the heat generation or absorption effects. Umavathi et al. [12] analysed the unsteady flow of two immiscible fluids through a horizontal channel with time-dependent oscillatory wall transpiration velocity. They observed that the flow and heat transfer characteristics in a horizontal channel can be controlled by considering different fluids having different viscosities, conductivities and also by varying the amplitude of the transpiration velocity at the boundary. An entropy generation and magnetic convection of CuO-water nanofluid in a C-shaped cavity subjected to a horizontal were studied by Chamkha et al. [13]. Parvin et al. [14] considered the steady laminar convection flow and heat transfer of Al_2O_3 – water nanofluid in an annulus. Parvin and Chamkha [15] presented the laminar convection and entropy generation of Cu – water nanofluid in a cavity with horizontal and vertical portion. They observed that the presence of nanofluid lowered the flow strength whereas raises the Nusselt number, entropy generation and Bejan number. Further studies include in [16-22].

In real life engineering applications such as solar collectors, heat exchanger with different shaped duct constructions the shape of the cavity can also be non-rectangular.

The study of convection flows in such geometries are difficult in comparison to the square enclosures due to the sloping walls of the non-rectangular enclosures. In general, the mesh nodes do not lie along the sloping walls, and consequently, the effort required for determining flow characteristics increases significantly. In trapezoidal enclosures, the aspect ratio of the cavity and the presence of the baffles along the walls play a prominent role in the flow and temperature distributions. The patterns within the complex enclosures are greatly dependent on the amplitude-wavelength ratio and the number of undulations of the wavy walls. The numerical simulations of natural convection heat transfer within the enclosures have been studied extensively with different numerical methods and various non-square enclosures. Basak et al. [23] reported the convective heat transfer within a right-angled triangular enclosure under the effects of thermal boundary conditions using the Galerkin finite element method. They studied the flow characteristics with various Prandtl number and Rayleigh number. Al-Mudhaf et al. [24] used the finite difference method to discuss the double-diffusive natural convection within trapezoidal enclosures filled with porous medium. They explored the heat and mass transfer characteristics inside the enclosure with Soret and Dufour effects. Erturk et al. [25] introduced a fine uniform grid mesh simulation of lid-driven cavity flow in a square enclosure with high Reynolds number, i.e., $Re = 21000$. They developed a finite difference scheme for cavity flows with second-order accuracy. Sarris et al. [26] reported the natural convection with sinusoidal heating of the top wall in a rectangular enclosure. They found that the depth of thermal penetration enhanced with aspect ratio.

Flow circulation and heat transfer characteristics were examined within porous rhombic annulus by Moukalled et al. [27] using a pressure-based finite volume method. Finite element simulation-based numerical investigation of natural convection within the porous trapezoidal enclosure was reported by Basak et al. [28]. Bairi et al. [29] discussed the 2D transient natural convection heat transfer within parallelogrammic enclosure both numerically and experimentally. Heatline based analysis of thermal transport and heat recovery within entrapped triangular cavities was reported by Basak et al. [30]. A finite-difference technique was employed by Sheremet et al. [31] to simulate the natural convection in entrapped triangular cavities filled with nanofluid. The researchers are interested in convective flows within the enclosures of different shapes. For instance, Baytas et al. [32] reported convective flows in a porous trapezoidal enclosure. The similar work is presented with ferrofluid [33].

The finite difference method (FDM), a well-known and most efficient technique used to solve problems related to fluid mechanics, heat transfer, chemical engineering processes, solid mechanics and many other fields. The pressure gradient is the major term in the momentum equation. Solving the incompressible flow equations are more complex with pressure gradient. Due to this researchers use some special techniques to solve the fluid flow equations. The pressure term is eliminated using the penalty method [23] and by stream function and vorticity formulation [34]. The detailed procedure with mathematical models was discussed by Das et al. [35]. Sheremet et al. [36] used a finite difference scheme and examined the natural convection in an inclined wavy-wall enclosure with Tiwari and Das' nanofluid model. Pressure correction (MAC Method) based numerical simulation of convective flows in an enclosure is conducted by many researchers [37–39]. Akbarzadeh and Fardi [40] presented the heat transfer analysis of free convection nanofluid flows with different properties in 2D and 3D channels with trapezoidal cross-sections using finite volume method and simpler algorithm. They considered the effects of nanoparticle volume fraction, Rayleigh number and sidewall angle on heat transfer performance. Al-Weheibi et al. [41] investigated numerically the

unsteady natural convection flow and heat transfer of nanofluid within a trapezoidal enclosure. A strong buoyancy force was observed with higher Rayleigh number. Basak et al. [42] analysed the natural convection heat transfer within the trapezoidal enclosures for the case of linearly heated sidewalls, and linearly heat left the wall and cold right wall with the top wall being adiabatic and bottom hot wall using the penalty finite element method. They graphically and numerically presented the streamlines, isotherms and heatlines for a wide range of Prandtl and Raleigh numbers. Almakhyoul [43] presented the numerical analysis of a steady natural convection flow within a trapezoidal enclosure with three different cases of thin baffles attached at the heated wall while the inclined wall is cooled and the horizontal walls are well-insulated.

Natural convection heat transfer flows in enclosures has been considered by many researchers in the past few years. In these studies, square, rectangular, inclined, slender and shallow cavities with various wall conditions have been considered extensively by different researchers. In various industrial applications such as solar collectors, nuclear reactors, heat exchangers and electronic equipment's, the heat transfer past a fluid layer within an enclosure has to be controlled. Despite several numerical studies on trapezoidal enclosures reported in the literature, there is still a serious lack of information regarding the problem of heat transfer enhancement in trapezoidal enclosures. The present numerical simulation aims to study the convective heat transfer in a trapezoidal enclosure. The computational physical domain with boundary conditions is shown in Figure 1. The graphical results are presented in the form of streamlines, isotherms, local and mean Nusselt numbers. Based on the survey of literature and authors' knowledge, the problem considered in this paper, i.e., natural convection within trapezoidal enclosure under the effects of various values of Prandtl number is discussed for the first time.

GEOMETRY DEFINITION AND BASIC EQUATIONS

Consider the buoyancy-driven the flow of a two-dimensional trapezoidal cavity. The schematic diagram of the present computational regime is depicted in Figure 1. The left sidewall of the enclosure is maintained at constant temperatures T_h whereas, the lower flat and right wall are thermally insulated. The upper inclined wall is maintained at constant temperatures T_c such that $T_h > T_c$. The thermophysical properties of the fluid flow field within the enclosure are assumed to be constant except the density variations causing a body force term in the momentum equation. It is also invoked that the influence of buoyancy is due to the Boussinesq approximation. The viscous dissipation and Joule heating effects are neglected. In line with [35-36, 41-42] and based on these assumptions, the conservation equations of mass, momentum and thermal energy can be written as follows:

Continuity,

$$\frac{\partial u}{\partial x} + \frac{\partial v}{\partial y} = 0 \quad (1)$$

Momentum equation in x-direction,

$$\rho_f \left(\frac{\partial u}{\partial t} + u \frac{\partial u}{\partial x} + v \frac{\partial u}{\partial y} \right) = -\frac{\partial p}{\partial x} + \mu_f \left(\frac{\partial^2 u}{\partial x^2} + \frac{\partial^2 u}{\partial y^2} \right) \quad (2)$$

Momentum equation in y-direction,

$$\rho_f \left(\frac{\partial v}{\partial t} + u \frac{\partial v}{\partial x} + v \frac{\partial v}{\partial y} \right) = - \frac{\partial p}{\partial y} + \mu_f \left(\frac{\partial^2 v}{\partial x^2} + \frac{\partial^2 v}{\partial y^2} \right) + \rho_f g \beta (T - T_c) \quad (3)$$

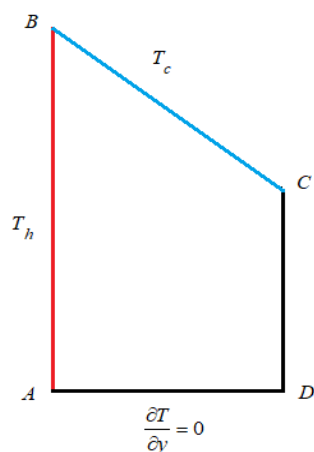
Energy equation,

$$\frac{\partial T}{\partial t} + u \frac{\partial T}{\partial x} + v \frac{\partial T}{\partial y} = \alpha_f \left(\frac{\partial^2 T}{\partial x^2} + \frac{\partial^2 T}{\partial y^2} \right) \quad (4)$$

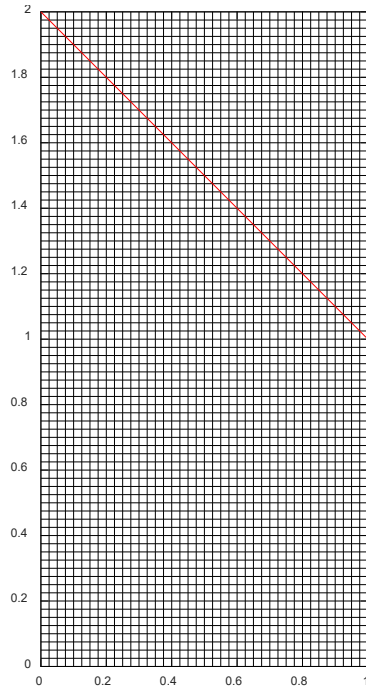
Here u and v are the velocity components along x - and y -axis respectively, g is the acceleration due to gravity, p is the pressure, β is the thermal expansion coefficient, T is temperature and α_f is thermal diffusivity. Introducing the dimensionless parameters as follows:

$$\tau = \frac{tu_0}{L}, \quad X = \frac{x}{L}, \quad Y = \frac{y}{L}, \quad U = \frac{u}{u_0}, \quad V = \frac{v}{u_0}, \quad \theta = \frac{T - T_c}{T_h - T_c}, \quad P = \frac{p}{u_0^2 \rho_f} \quad (5)$$

$$u_0 = \frac{\alpha}{L}$$



(a)



(b)

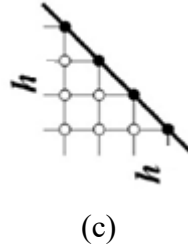


Figure 1. (a) Geometry, (b) utilised mesh and (c) boundary conditions.

Using Equation (5) in Equation (1) to (4), the transformed dimensionless governing equations are:

$$\frac{\partial U}{\partial X} + \frac{\partial V}{\partial Y} = 0 \quad (6)$$

$$\frac{\partial U}{\partial \tau} + U \frac{\partial U}{\partial X} + V \frac{\partial U}{\partial Y} = -\frac{\partial P}{\partial X} + \text{Pr} \left(\frac{\partial^2 U}{\partial X^2} + \frac{\partial^2 U}{\partial Y^2} \right) \quad (7)$$

$$\frac{\partial V}{\partial \tau} + U \frac{\partial V}{\partial X} + V \frac{\partial V}{\partial Y} = -\frac{\partial P}{\partial Y} + \text{Pr} \left(\frac{\partial^2 V}{\partial X^2} + \frac{\partial^2 V}{\partial Y^2} \right) + Ra \cdot \text{Pr} \theta \quad (8)$$

$$\frac{\partial \theta}{\partial \tau} + U \frac{\partial \theta}{\partial X} + V \frac{\partial \theta}{\partial Y} = \left(\frac{\partial^2 \theta}{\partial X^2} + \frac{\partial^2 \theta}{\partial Y^2} \right) \quad (9)$$

Where X, Y are dimensionless Cartesian coordinates. U and V are dimensionless velocity in x and y -direction respectively, P is the dimensionless pressure, θ is the dimensionless temperature and T_h and T_c are the temperatures of the vertical walls. Ra and Pr are Rayleigh and Prandtl numbers respectively and are defined as:

$$Ra = \frac{g\beta(T_h - T_c)(1 - C_c)L^3}{\nu_f^2}, \quad \text{Pr} = \frac{\nu_f}{\alpha_f}$$

Dimensionless stream function ψ and vorticity ω are defined as:

$$U = \frac{\partial \psi}{\partial Y}, \quad V = -\frac{\partial \psi}{\partial X} \quad (10)$$

$$\omega = \frac{\partial V}{\partial X} - \frac{\partial U}{\partial Y} \quad (11)$$

$$\omega = -\frac{\partial^2 \psi}{\partial X^2} - \frac{\partial^2 \psi}{\partial Y^2}$$

Vorticity transport equation is obtained from the differentiation of x -momentum equation with respect to y and y -momentum equation with respect to x and then subtracting them, we get.

$$\frac{\partial \omega}{\partial \tau} + U \frac{\partial \omega}{\partial X} + V \frac{\partial \omega}{\partial Y} = \text{Pr} \left(\frac{\partial^2 \omega}{\partial X^2} + \frac{\partial^2 \omega}{\partial Y^2} \right) + Ra \cdot \text{Pr} \frac{\partial \theta}{\partial X} \tag{12}$$

The boundary conditions shown in Figure 1 are as follows:

$$\theta = 0 \text{ on the upper slant wall (BC)}$$

$$\theta = 1 \text{ on the left vertical wall (AB)}$$

$$\frac{\partial \theta}{\partial n} = 0 \text{ on the other walls (CD \& AD)}$$

The vorticity on the boundary of the trapezoidal enclosure are calculated from the stream function formulation and the known conditions of velocity during the iterative solution procedure. The local and average heat transfer rates are defined respectively as:

$$Nu = - \left(\frac{\partial \theta}{\partial X} \right)_{X=0} \text{ and } Nu_M = - \int_0^1 \left(\frac{\partial \theta}{\partial X} \right) dY$$

SOLUTION PROCEDURE

A regular uniform grid distribution is used as shown in Figure 1(b). The inclined walls were approximated with staircase-like zigzag lines. This technique is adopted based on the study [44]. In order to test the grid-independency of the present numerical solution, different uniform mesh combinations were examined for $Ra = 10^3$ and $Pr = 0.71$ as presented in Table 1. The average Nusselt number of the heated wall is calculated in order to reach grid independence. It is concluded that a grid size of 81×41 ensures a grid-independent solution.

Table 1. Comparison of the average Nusselt number Nu_M along the heated wall for different mesh sizes for $Ra = 10^3$ and $Pr = 0.7$.

Mesh size	21×41	41×81	81×161	101×201	121×241
Nu_M	2.62511	3.051232	3.05323	3.05292	3.06062

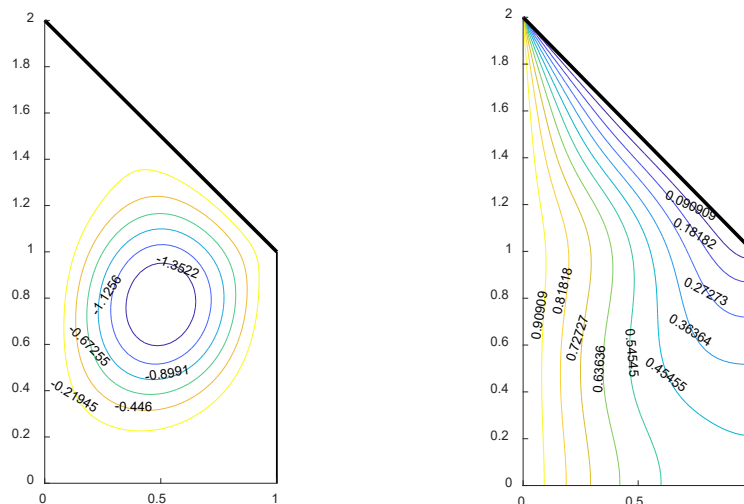
The governing dimensionless partial differential Eq. (9), (11) and (12) with appropriate boundary conditions are solved by the well-known finite difference method. A uniform fine grid system is considered. The second-order finite difference approximation and central difference approximation are used for convective and diffusion terms respectively. The transient approximation Eq. (9) and (12) are solved using the time integration scheme while the Poisson Eq. (11) is computed by the well-known Gauss-seidel iterative method with slandered five-point formula. The time integration is

terminated when each computed parameter (stream function, vorticity and temperature) reaches the relaxation bellow 10^{-8} .

RESULTS AND DISCUSSION

Natural convection of heat transfer in a trapezoidal enclosure with various Prandtl number is examined numerically using a finite difference method. The four walls of the enclosure are maintained at various wall temperatures. The numerical calculations are carried out for various values of Rayleigh number ($Ra = 10^3 - 10^5$) and Prandtl number ($Pr = 0.025, 0.71$ and 10). Flow pattern, isotherms, local and average Nusselt number for different values Ra and Pr are presented in Figure 2 to 8. Regardless of Rayleigh number and Prandtl number values a single enlarged convective eddy is developed inside the enclosure illustrating the appearance of raising flows along the left wall of the cavity and descending flows close to the uniform cold inclined wall (Figure 2 to 4). The fluid flow inside an enclosure circulates in a clockwise direction while the circular shape of the eddy is developed inside the enclosure for $Pr = 0.025$ and $Ra = 10^3$ as seen in Figure 2(a). The circular shape is shifted to elliptical circulation for increasing of Pr . The isotherms contours are parallel to vertical walls for $Ra = 10^5$ and $Pr = 10$. The isotherm patterns divert and move towards cold portion for decreasing values of Pr .

Figure 3 illustrates the influence of Pr on convective flow within the trapezoidal enclosure for $Ra = 10^4$. The Prandtl number is varied from 0.025 to 10 . The fluid flow within the enclosure is formed with different shapes for different Pr values. The flow rate is increased by enhancing Rayleigh number ($Ra = 10^4$). The mono enlarged circular cell appears inside the enclosure for $Pr = 0.025$ and the corresponding isotherms are shifted from parallel to curvy nature. The isotherms with wavier nature are noticed in the middle of enclosure for low Prandtl number. The wavy nature of isotherms diminish for increasing of Pr values (i.e. $Pr = 0.71$ and 10). The circular cell gradually shifts to elliptical shape by enhancing Pr from 0.71 to 10 . The thermal boundary layer is formed along the cold wall and hot wall with increasing values of Pr .



(a)

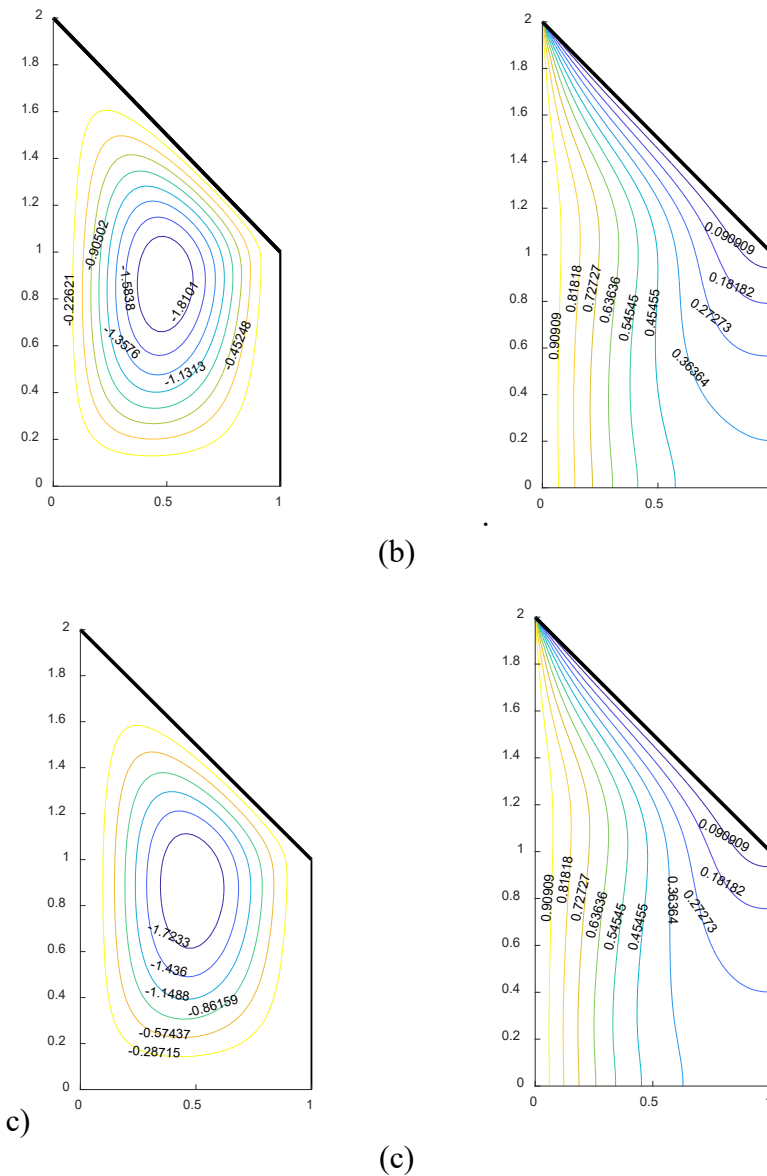
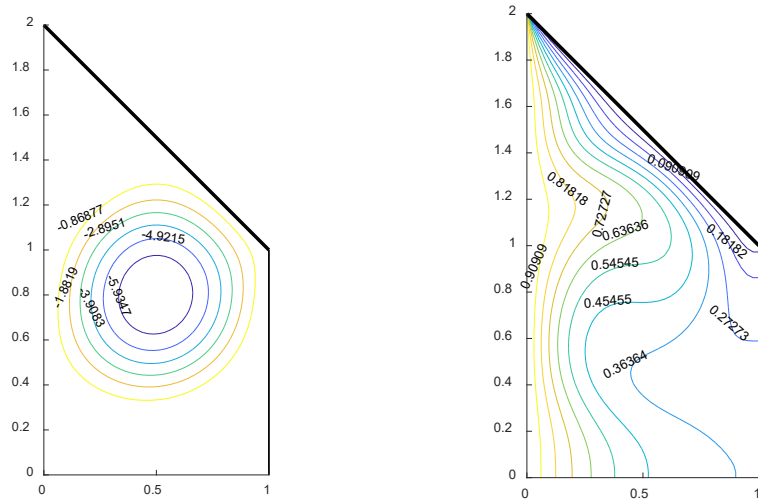


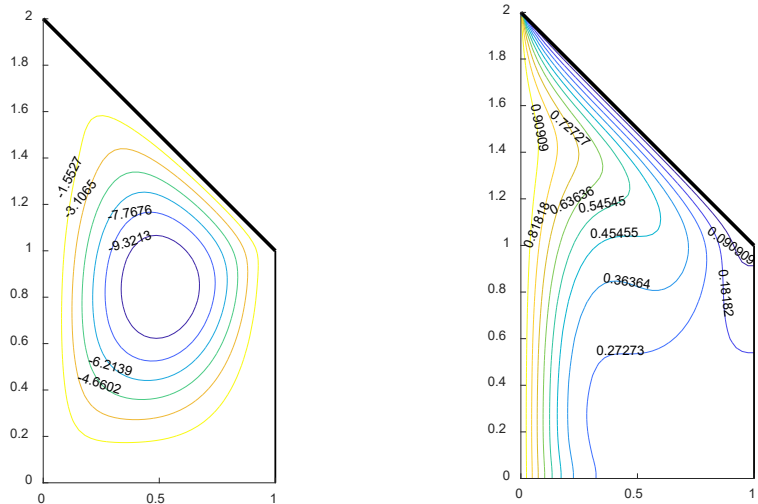
Figure 2. Streamlines and isotherms for $Ra=10^3$ at (a) $Pr=0.025$, (b) $Pr=0.71$, (c) $Pr=10$.

The effects of Pr on flow pattern and isotherms for $Ra = 10^5$ are depicted in Figure 4. The flow patterns gradually change with different values of Pr (i.e. $Pr = 0.025, 0.71$ and 10). Two convective cells are developed within the trapezoidal enclosure for $Pr = 0.025$. The larger convective cell is developed in the middle while the minor appears at top of the enclosure. The surrounds of isotherms are observed inside the enclosure for $Pr = 0.025$. As Pr is increased, the surrounds of isotherms shift to straight lines and the circular convective cell transform to an elliptical shaped cell. A strong thermal boundary layer is developed along the cold and hot wall for $Pr = 10$.

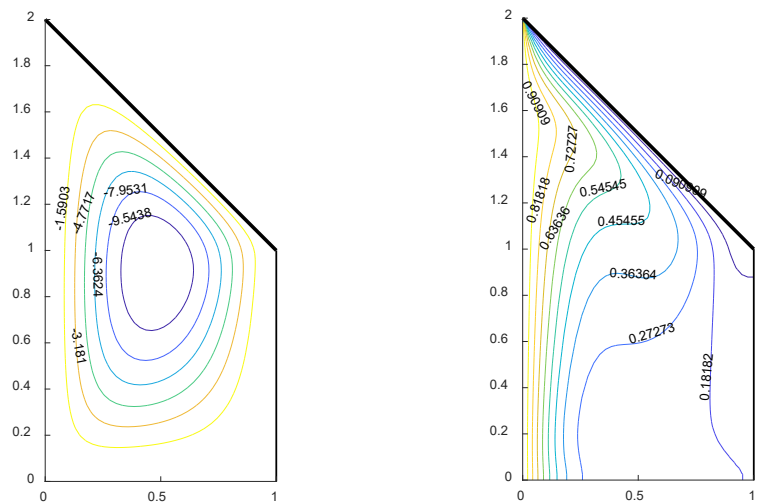
Simulation of Natural Convection Heat Transfer in a 2-D Trapezoidal Enclosure



(a)

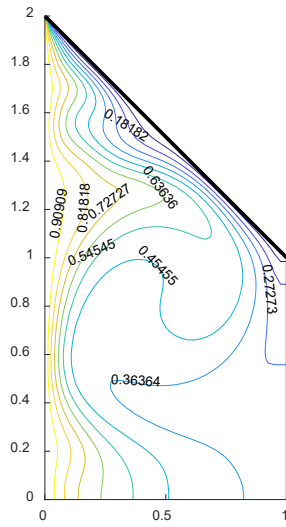
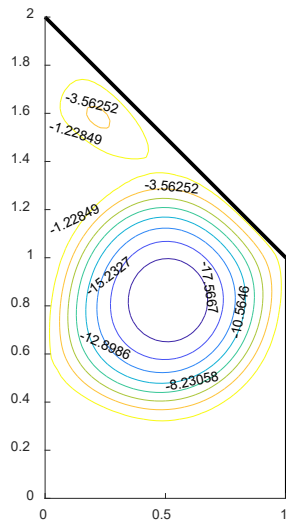


(b)

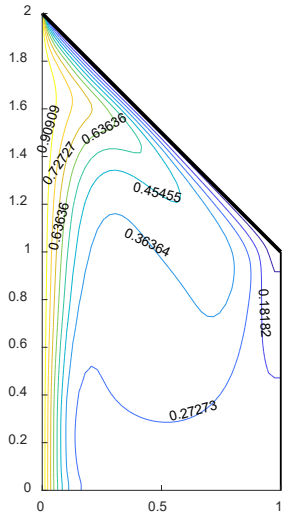
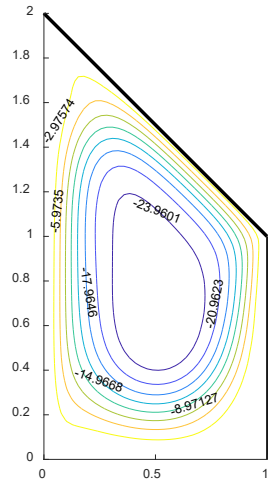


(c)

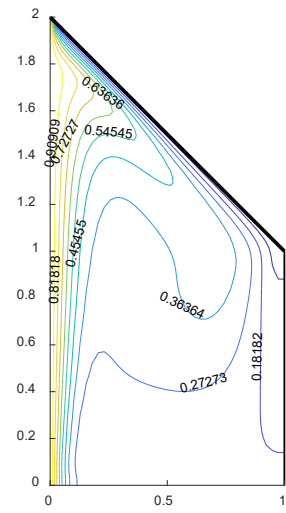
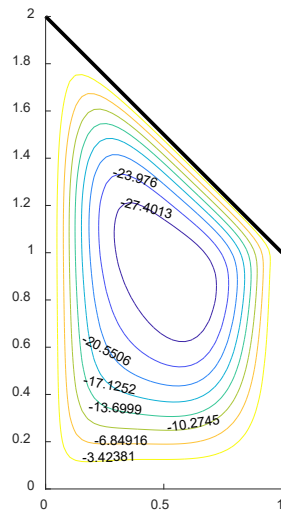
Figure 3. Streamlines and isotherms for $Ra=10^4$ at (a) $Pr=0.025$, (b) $Pr=0.71$, (c) $Pr=10$.



(a)



(b)



(c)

Figure 4. Streamlines and isotherms for $Ra=10^5$ at (a) $Pr=0.025$, (b) $Pr=0.71$, (c) $Pr=10$.

Figure 5(a) depicts the profiles of local Nusselt number along the vertical isothermal hot wall for various values of Ra with Pr fixed at 0.025. Regardless of Rayleigh number, the rate of heat transfer is more at top of the hot wall. An increase in Ra leads to an increase in the heat transfer rate. The local Nusselt number increases monotonically for low Rayleigh number $Ra = 10^3$. With the enhance of Ra ($Ra = 10^4$ and $Ra = 10^5$), the local Nusselt number is seen to increase non-uniformly.

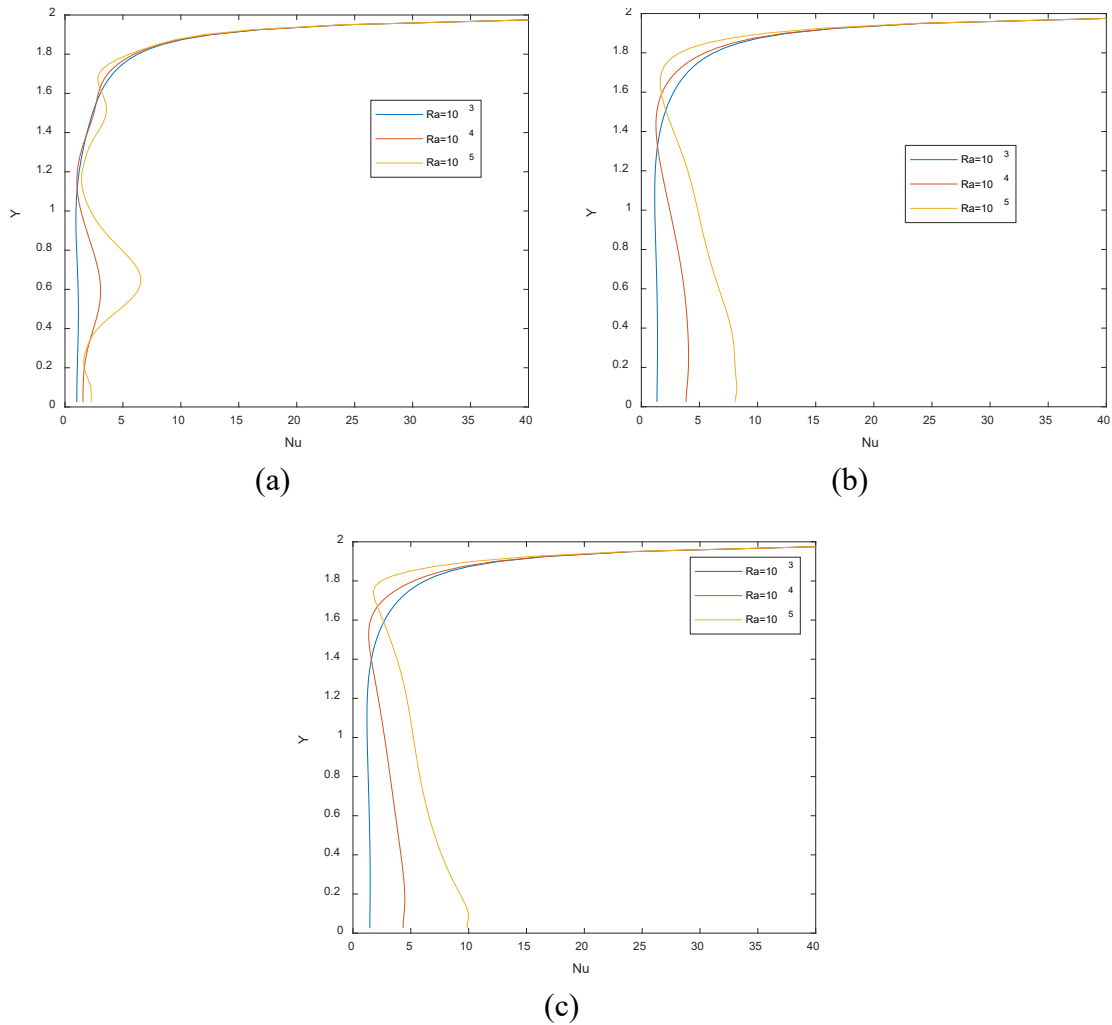


Figure 5. Local Nusselt number of hot wall for different values of Ra at (a) $Pr = 0.025$, (b) $Pr = 0.71$ and (c) $Pr=10$.

Figure 5(b) and 5(c) demonstrate the effects of Rayleigh number on local Nusselt number along the hot wall for $Pr = 0.71$ and $Pr = 10$ respectively. The local Nusselt number is observed to increase more at bottom of the hot wall for $Ra = 10^4$ and $Ra = 10^5$ while the rate of heat transfer decreases towards the upward except at top portion of hot wall. Regardless of the Prandtl number, the local Nusselt number is seen to gradually increase along the left isothermal hot wall and abundant heat transfer rate is observed at top of the hot wall for $Ra = 10^3$. The fluid flow rate is seen to increase with increasing Ra . The influence of Pr on local Nusselt number of the hot wall with $Ra = 10^5$ is presented in Figure 6. The local Nusselt number of hot wall is seen to gradually reduce from bottom

of the wall to the top wall except at the top corner of hot wall for $Pr = 0.71$ and $Pr = 10$. For $Pr = 0.025$, the heat transfer rate is seen to raise nonlinearly from bottom to top of wall due to the fluid flow which circulates circularly below the slant wall in the enclosure. The average Nusselt number of the hot wall with various values of Ra is presented in Figure 7. The average Nusselt number of hot wall is seen to gradually increases with augment of Ra . Comparatively for $Pr = 0.71$, $Pr = 0.025$ and $Pr = 10$, the heat transfer rate is raises when increasing of Ra , In addition the more heat transfer rate registered at $Pr = 10$.

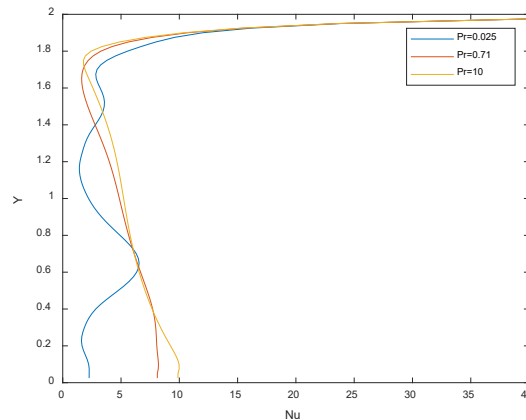


Figure 6. Local Nusselt number of hot wall for different values of Pr for $Ra = 10^5$.

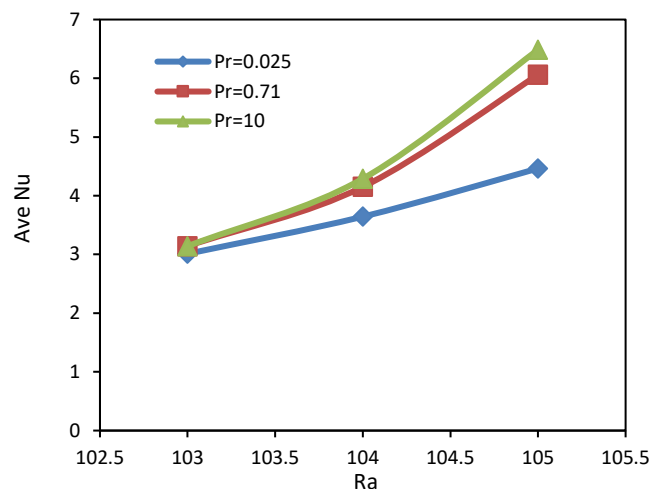


Figure 7. Average Nusselt number of hot wall for different values of Pr .

CONCLUSION

Natural convective flow in a trapezoidal enclosure with cold inclined top wall, isothermal hot left vertical wall and rest of the wall are adiabatic has been examined numerically. The Numerical analysis of the fluid flow patterns and rate of heat transfer is studied for a wide range of Rayleigh number, $Ra = 10^3 - 10^5$ and Prandtl number, $Pr = 0.025, 0.71$ and 10 . The results are as follows:

- i. A mono enlarged convective cell is developed inside the trapezoidal enclosure for various values of Rayleigh number with $Pr = 0.71$ and $Pr = 10$. The fluid flow rate and rate of heat transfer are the enhancing functions of the Rayleigh number.

- ii. Regardless of Rayleigh number, the convective cell is developed in the circular form inside the enclosure for the low value of Prandtl number (*i.e.* $Pr = 0.025$).
- iii. An increase in Prandtl number leads to heat transfer enhancement and the thermal boundary layer intensification of slant wall for high values of Ra ($Ra = 10^5$).
- iv. The rate of heat transfer is analysed with the local Nusselt number of the hot wall. For $Pr = 10$ with $Ra = 10^5$, the uniform heating of left vertical wall exhibits a higher heat transfer rate.
- v. Regardless of the Rayleigh number, the local Nusselt number exhibits nonlinear enhancement for the low value of Prandtl number ($Pr = 0.025$).
- vi. Heat transfer rate is greater at the top corner of hot wall while the local Nusselt number gradually reduces from bottom to top of the hot wall and is suddenly enhanced as we move close to the top corner of the wall.
- vii. Regardless of the Prandtl number, the average Nusselt number exhibits significant enhancement for increasing Rayleigh number.

REFERENCES

- [1] Ostrach S. Natural convection in enclosures. *Journal of Heat Transfer*, 1988; 110: 1175–1190.
- [2] Iyican L. Natural convection heat transfer in trapezoidal enclosures. Ph.D. dissertation. University of Houston. Dec. 1979.
- [3] Iyican L, Bayazitoglu Y, and Witte LC. An analytical study of natural convection heat transfer within a trapezoidal enclosure. *Journal of Heat Transfer*, 1980; 102(4): 640-647.
- [4] Iyican L, Bayazitoglu Y. An experimental study of natural convection in trapezoidal enclosures. *Journal of Heat Transfer*, 1980; 102(4): 648-653.
- [5] Basak T, Roy S, Pop I. Heat flow analysis from natural convection within trapezoidal enclosures based on heatline concept. *International Journal of Heat and Mass Transfer*, 2009; 59: 2471-2483.
- [6] Esfe MH, Arani AAA, Yan WM, Ehteram H, Aghaie A, Afrand M. Natural convection in a trapezoidal enclosure filled with carbon nanotube–EG–water nanofluid. *International Journal of Heat and Mass Transfer*, 2016; 92: 76-82.
- [7] Ismael MA, Chamkha AJ. Conjugate natural convection in a differentially heated composite enclosure filled with a nanofluid. *Journal of Porous Media*, 2015; 18(7): 699-716.
- [8] Ali J, Chamkha, Al-Naser H. Hydromagnetic double-diffusive convection in a rectangular enclosure with uniform side heat and mass fluxes and opposing temperature and concentration gradients. *International Journal of Thermal Science*, 2004; 41: 936-948.
- [9] Ben-Nakhi A, Chamkha AJ. Conjugate natural convection in a square enclosure with inclined thin fin of arbitrary length. *International Journal of Thermal Science*, 2007; 46: 467-478.
- [10] Adu-Nada E, Chamkha AJ. Mixed convection flow of a nanofluid in a lid-driven cavity with a wavy wall. *International Communications in Heat and Mass Transfer*, 2014; 57: 36-47.
- [11] Chamkha AJ. Double-diffusive convection in a porous enclosure with cooperating temperature and concentration gradients and heat generation or absorption effects. *Numerical Heat Transfer, Part A: Applications: An International Journal of Computation and Methodology*, 2002; 41:1: 65-87.

- [12] Umavathi JC, Chamkha AJ, Mateen A, Al-Mudhaf A. Unsteady two-fluid flow and heat transfer in a horizontal channel. *Heat and Mass Transfer*, 2005; 48: 81-90.
- [13] Chamkha AJ, Ismael M, Kasaeipoor A, Armaghani T. Entropy generation and natural convection of CuO-water nanofluid in C-shaped cavity under magnetic field. *Entropy*, 2016; 18(2): 50.
- [14] Parvin S, Nasrin R, Alim MA, Hossain NF, Chamkha AJ. Thermal conductivity variation on natural convection flow of water-alumina nanofluid in an annulus. *International Journal of Heat and Mass Transfer*, 2012; 55(19-20): 5268-5274.
- [15] Parvin S, Chamkha AJ. An Analysis on free convection flow, heat transfer and entropy generation in an odd-shaped cavity filled with nanofluid. *International Communications in Heat and Mass Transfer*, 2014; 54: 8-17.
- [16] Muneer A. Ismael, Armaghani T, Chamkha AJ. Conjugate heat transfer and entropy generation in a cavity filled with a nanofluid-saturated porous media and heated by a triangular solid. *Journal of Taiwan Institute of Chemical Engineers*, 2016; 59: 138-151.
- [17] Ismael MA, Pop I, Chamkha AJ. Mixed convection in a lid-driven square cavity with partial slip. *International Journal of Thermal Sciences*, 2014; 82: 47-61.
- [18] Nasrin R, Alim MA, Chamkha AJ. Combined convection flow in triangular wavy chamber filled with water-cuo nanofluid: effect of viscosity models. *International Communications in Heat and Mass Transfer*, 2012; 39(8): 1226-1236.
- [19] Chamkha AJ, Miroshnichenko IV, Sheremet MA. Numerical analysis of unsteady conjugate natural convection of hybrid water-based nanofluid in a semi-circular cavity. *Journal of Thermal Science and Engineering Applications*, 2017; 9(4): 041004.
- [20] Chamkha AJ, Abu-Nada E. Mixed convection flow in single- and double-lid driven square cavities filled with water-al₂o₃ nanofluid: effect of viscosity models. *European Journal of Mechanics – B/Fluids*, 2012; 36: 82-96.
- [21] Ben-Nakhi A, Chamkha AJ. Effect of length and inclination of a thin fin on natural convection in a square enclosure. *Numerical Heat Transfer, Part A: Applications: An International Journal of Computation and Methodology*, 2006; 50(4): 381-399.
- [22] Chamkha AJ, Al-Naser H. Hydromagnetic double-diffusive convection in a rectangular enclosure with uniform side heat and mass fluxes and opposing temperature and concentration gradients. *International Journal of Thermal Sciences*, 2002; 41: 936-948.
- [23] Basak T, Roy S, Thirumalesha Ch. Finite element analysis of natural convection in a triangular enclosure: Effects of various thermal boundary conditions. *Chemical Engineering Science*, 2007; 62: 2623 – 2640.
- [24] Al-Mudha AF, Rashad AM, Ahmed SE, Chamkha AJ, EL-Kabeir SMM. Soret and Dufour effects on unsteady double diffusive natural convection in porous trapezoidal enclosures. *International Journal of Mechanical Sciences*, 2018; 140: 172–178.
- [25] Erturk E, Corke TC, Gokcol C. Numerical solutions of 2-D steady incompressible driven cavity flow at high Reynolds numbers. *International Journal of Numerical Methods and Fluids*, 2005; 48: 747–774.
- [26] Sarris IE, Lekakis I, Vlachos NS. Natural convection in a 2-D enclosure with sinusoidal upper wall temperature. *Numerical Heat Transfer Applications*, 2002; 42(5): 513–530.
- [27] Moukalled F, Darwish M. Natural convection heat transfer in a porous rhombic annulus. *Numerical Heat Transfer Applications*, 2010; 58: 101–124.
- [28] Basak T, Roy S, Singh A, Pop I. Finite element simulation of natural convection flow in a trapezoidal enclosure filled with porous medium due to uniform and non-uniform heating. *International Journal of Heat and Mass Transfer*, 2009; 52: 70–78.

- [29] Bairi A, Garcia de Maria JM, Laraqi N. Transient natural convection in parallelogrammic enclosures with isothermal hot wall. Experimental and numerical study applied to on-board electronics, Applications in Thermal Engineering, 2010; 30: 1115–1125.
- [30] Basak T, Aravind G, Roy S, Balakrishnan AR. Heatline analysis of heat recovery and thermal transport in materials confined within triangular cavities. International Journal of Heat and Mass Transfer, 2010; 53: 3615–3628.
- [31] Sheremet MA, Revnic C, Pop I. Natural convective heat transfer through two entrapped triangular cavities filled with a nanofluid: Buongiorno's mathematical model. International Journal of Mechanical Science, 2017; 133: 484–494.
- [32] Baytas AC, Pop I. Natural convection in a trapezoidal enclosure filled with a porous medium. International Journal of Engineering Science, 2001; 39: 125–134.
- [33] Sheikholeslami M, Vajravelu K, Rashidi MM. Forced convection heat transfer in a semi annulus under the influence of a variable magnetic field. International Journal of Heat and Mass Transfer, 2016; 92: 339–348.
- [34] Ali J. Chamkha, Igor V. Miroshnichenko, Mikhail A. Sheremet. Unsteady Conjugate Natural Convective Heat Transfer and Entropy Generation in a Porous Semicircular Cavity. Journal of Heat Transfer, 2018; 140: 1-19.
- [35] Das D, Roy M, Basak T. Studies on natural convection within enclosures of various (non-square) shapes – A review. International Journal of Heat and Mass Transfer, 2017; 106: 356–406.
- [36] Sheremet MA, Trîmbițaș R, Groșan T, Pop I. Natural convection of an alumina-water nanofluid inside an inclined wavy-walled cavity with a non-uniform heating using Tiwari and Das'nanofluid model: Applied Mathematics and Mechanics, 2018; 39(10): 1425-1436.
- [37] Venkatadri K, GouseMohiddin S, Suryanarayana RM. Mathematical modelling of unsteady MHD double diffusive natural convection flow in a square cavity. Frontiers in Heat and Mass Transfer (FHMT), 2017; 9: 33.
- [38] Venkatadri K, GouseMohiddin S, Suryanarayana RM. Hydromagneto quadratic natural convection on a lid driven square cavity with isothermal and non-isothermal bottom wall. Engineering Computations, 2017; 34(8): 2463-2478.
- [39] Hidayathulla Khan. BMD, Venkatadri K, Beg OA, Ramachandra Prasad V, Mallikarjuna B. Natural convection in a square cavity with uniformly heated and/or insulated walls using marker-and-cell method. International Journal of Applied and Computational Mathematics, 2018; 4 (61).
- [40] Akbarzadeh P, Fardi AH. Natural convection heat transfer I 2-D and 3-D trapezoidal enclosure filled with nanofluid. Journal of Applied Mechanics and Technical Physics, 2018; 59(2): 292-302.
- [41] Al-Weheibi SM, Rahman MM, Alam MS, Vajravelu K. Numerical simulation of natural convection heat transfer in a trapezoidal enclosure filled with nanoparticles. International Journal of Mechanical Sciences, 2017; 131–132: 599–612.
- [42] Basak T, Ramakrishna D, Roy S, Matta A, I. Pop. A comprehensive heatline based approach for natural convection flows in trapezoidal enclosures: effect of various walls heating. International Journal of Thermal science, 2011; 50(8): 1385-1404.
- [43] Almkhyoul ZM. Natural convection heat transfer in trapezoidal enclosure with baffles attached to heated wall. Al-Rafidan Engineering, 2014; 22(3): 2014.
- [44] Gibanov NS, Sheremet MA, Pop I. Free convection in a trapezoidal cavity filled with a micropolar fluid. International Journal of Heat and Mass Transfer, 2016; 99: 831-838.